

The time-lag – photon-index correlation in GX 339–4

Nikolaos D. Kylafis^{1,2} and Pablo Reig^{2,1}

¹ University of Crete, Physics Department & Institute of Theoretical & Computational Physics, 70013 Heraklion, Crete, Greece

² IESL & Institute of Astrophysics, Foundation for Research and Technology-Hellas, 71110 Heraklion, Crete, Greece

Received ; Accepted ;

ABSTRACT

Context. Black-hole transients, as a class, exhibit during their outbursts a correlation between the time lag of hard photons with respect to softer ones and the photon index of the hard X-ray power law. The correlation is not very tight and therefore it is necessary to examine it source by source.

Aims. The objective of the present work is to investigate in detail the time-lag – photon-index correlation in GX 339-4, which is the best studied black-hole transient.

Methods. We have obtained *RXTE* energy spectra and light curves and have computed the photon index and the time lag of the 9 – 15 keV photons with respect to the 2 – 6 keV ones. The observations cover the first stages of the hard state, the pure hard state, and the hard-intermediate state.

Results. We have found a tight correlation between time lag and photon index Γ in the hard and hard-intermediate states. At low Γ , the correlation is positive and it becomes negative at large Γ . By assuming that the hard X-ray power law index Γ is produced by inverse Compton scattering of soft disk photons in the jet, we have reproduced the entire correlation by varying two parameters in the jet: the radius of the jet at its base R_0 and the Thomson optical depth along the jet τ_{\parallel} . We have found that, as the luminosity of the source increases, R_0 initially increases and then decreases. This behavior is expected in the context of the Cosmic Battery.

Conclusions. Our jet model nicely explains the correlation with reasonable values of the parameters R_0 and τ_{\parallel} . These parameters also correlate between themselves. As a further test of our model, we predict the break frequency in the radio spectrum as a function of the photon index during the rising part of an outburst.

Key words. accretion, accretion disks – X-ray binaries: black holes – jets – X-ray spectra – X-ray timing – magnetic fields

1. Introduction

Despite the fact that significant progress has been made in the phenomenology and modelling of the X-ray emission of black-hole transients (BHTs) in the last decade, the accretion/ejection phenomena in these systems are still poorly understood. Understanding the emitted spectra is extremely important, because it reveals the physical processes giving rise to the high-energy radiation. However, at present, the knowledge that we can obtain is limited because there are more ways than one to reproduce the observed spectra (Titarchuk 1994; Esin et al. 1997; Poutanen & Fabian 1999; Reig et al. 2003; Markoff et al. 2005; Done et al. 2007). Timing properties add a new view of the sources and may help breaking the degeneracy inherent in the spectral analysis, but again there are various ways to explain the observations (Poutanen & Fabian 1999; Böttcher & Liang 1999; Kotov et al. 2001; Reig et al. 2003; Arévalo & Uttley 2006; Kroon & Becker 2016).

The way forward must come from the combination of spectral and timing information. Stringent constraints to the models come from the correlated timing and spectral behavior (Pottschmidt et al. 2003; Shaposhnikov & Titarchuk 2009; Reig et al. 2013; Stiele et al. 2013; Shidatsu et al. 2014; Grinberg et al. 2014; Kalamkar et al. 2015; Altamirano & Méndez 2015; Reig & Kylafis 2015; Reig et al. 2018; Axelsson & Done 2018) Hence, to make progress in our understanding of the accretion/ejection phenomena in BHTs, the observations must uncover these correlations and the models

must explain them and make predictions that can either verify or disprove the models.

Recently, we examined the BHTs as a class and found a correlation between the photon number spectral index Γ of the hard X-rays and the timelag t_{lag} of the 9 - 15 keV photons with respect to the 2 - 6 keV ones (Reig et al. 2018). Although the correlation is statistically significant, it shows large scatter, because the geometry and the physical properties of the comptonizing region are not the same in all BHTs. Consequently, a closer examination of each individual source may give more insights into the ongoing processes. We will address the scatter of the correlation in a subsequent paper (Reig & Kylafis, in preparation). In this work we start the individual investigation of the sources with GX 339-4. This source has exhibited several outbursts and it is one of the best studied BHTs.

The structure of this Letter is as follows: in § 2 we present the observations and the data analysis, in § 3 we describe briefly our jet model, in § 4 we compare the model with the observations and make a theoretical prediction, in § 5 we comment on our findings, and in § 6 we draw our conclusions.

2. Observations and data analysis

This study was performed using archival data of GX 339–4 from the Rossi X-ray Timing Experiment (*RXTE*). During the time that the mission was operational, GX 339-4 exhibited four major X-ray outbursts (Fig. 1, top panel). In this Letter, we focus on the 2006–2007 outburst because it presents the best statistics and the best sampled hard-intermediate state, which allow

us to explore the upper branch of the q -diagram in detail (Fig. 1, middle panel). However it should be noted that the shape of the correlation examined in this Letter is similar in all outbursts, as it can be seen in the bottom panel of Fig. 1 (see also Fig. 6 in Altamirano & Méndez 2015).

The details of the data analysis can be found in Reig et al. (2018). Here we briefly summarize the data products that we have used. To compute the time lags, we generated light curves $x_i(t)$ with time bin size 2^{-7} s in the energy ranges 2–6 keV (soft band) and 9–15 keV (hard band). We calculated an average cross vector $\langle C(\nu_j) \rangle = \langle X_1^*(\nu_j) X_2(\nu_j) \rangle$, where $X_i(\nu_j)$ are the Fourier transforms of light curves $x_i(t)$ and the asterisk denotes complex conjugate. The average was performed over multiple adjacent 64-s segments. The final time lag of the 9 – 15 keV photons with respect to the 2 – 6 keV ones resulted from the average of the time lags in the frequency range 0.05–5 Hz. The selection of the energy and frequency ranges was driven by the instrument sensitivity and signal-to-noise.

The spectral analysis was performed in the energy range 2–25 keV¹. We obtained the energy spectra using the standard-2 mode of the *RXTE* PCA instrument. To characterize the spectral continuum, we used an absorbed broken power law model. The hydrogen column density was fixed to $N_H = 4 \times 10^{21} \text{ cm}^{-2}$ (Dunn et al. 2010). A narrow Gaussian component (line width $\sigma \lesssim 0.9 \text{ keV}$) was added to account for the iron emission line at around 6.4 keV. The photon index used in our analysis is the one that corresponds to the hard power law, that is, after the break.

3. Jet model

Over the years, we have developed a simple jet model that explains the spectral and timing observations of BHTs quite well (Reig et al. 2003; Giannios et al. 2004; Giannios 2005; Kylafis et al. 2008; Reig & Kylafis 2015; Reig et al. 2018). The model used here is the same as that of Reig & Kylafis (2015) and Reig et al. (2018). The reader is referred to these papers for details. Here, we give only a brief description.

We assume a parabolic jet with a finite acceleration region. The electrons in the jet have a component of their velocity v_{\parallel} parallel to the axis of the jet and one perpendicular v_{\perp} to it. This is justified if the electrons in the jet have a steep power-law distribution in their Lorentz factors (Giannios 2005).

The accretion flow around the black hole consists of an inner hot flow and an outer geometrically thin accretion disk (Esin et al. 1997; Kylafis & Belloni 2015). The jet is fed by the hot inner flow, while the thin accretion disk is the source of blackbody photons at the base of the jet. These soft photons, either escape unscattered or are scattered in the jet and have on average their energy increased. This upscattering of the soft blackbody photons produces the hard X-ray power law with index Γ . Furthermore, this upscattering causes an average timelag of the harder photons with respect to the softer ones.

The parameters of the model are: the optical depth τ_{\parallel} along the axis of the jet, the radius of the jet R_0 at its base, the minimum Lorentz factor $\gamma = 1/\sqrt{1 - (v_0^2 + v_{\perp}^2)/c^2}$ of the electrons

¹ In Reig et al. (2018), we used both PCA and HEXTE data. The power-law index there is systematically lower by ~ 0.2 due to the different energy range used in the fits.

² The electrons in jets are believed to obey a power-law distribution in Lorentz γ ($dN/d\gamma \propto \gamma^{-\alpha}$), from some γ_{\min} to some γ_{\max} . Because of the steepness of this distribution ($\alpha \gtrsim 2$), most of the electrons in the jet have Lorentz gamma factors close to γ_{\min} . For simplicity, we have taken all the electrons to have $\gamma = \gamma_{\min}$.

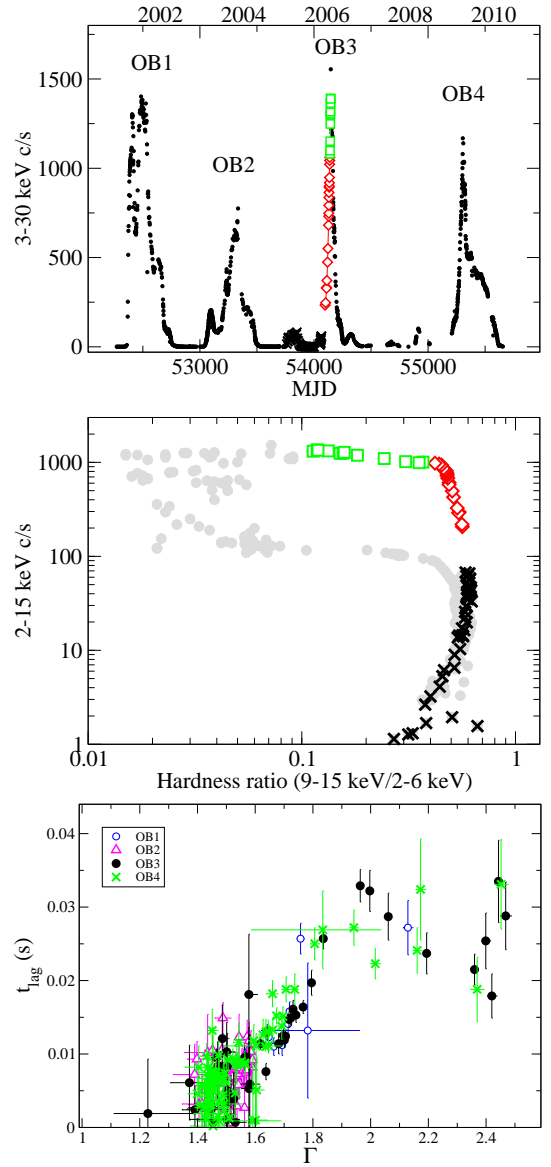


Fig. 1. *Top panel:* Long-term light curve of GX 339–4 showing four major X-ray outbursts. *Middle panel:* Hardness-intensity diagram for the 2006–2007 outburst. *Bottom panel:* Time lag between 9 – 15 keV photons with respect to 2 – 6 keV photons against the photon index of the hard power-law continuum. All four outbursts are included.

in the jet, the distance z_0 of the bottom of the jet from the black hole, the total height H of the jet, the temperature T_{bb} of the soft-photon input and the size z_1 and exponent p of the acceleration zone $v_{\parallel}(z) = (z/z_1)^p v_0$, for $z \leq z_1$, and $v_0 = v_{\parallel}(z)$ for $z > z_1$. The energy spectra, from which we derive the photon index Γ , and the time lag t_{lag} have been computed by Monte Carlo (Reig & Kylafis 2015; Reig et al. 2018).

4. Comparison of the model with the observations

In Fig. 2 (see also the bottom panel of Fig. 1), we show the average time lag t_{lag} as a function of the spectral index Γ for the 2006–2007 outburst. The filled circles give the observations and the rest of the symbols represent the model results as follows: For $\Gamma \lesssim 1.6$ the source is considered to be in the first stages of the hard state (black crosses in Fig. 2), for $1.6 \lesssim \Gamma \lesssim 1.9$ the source is

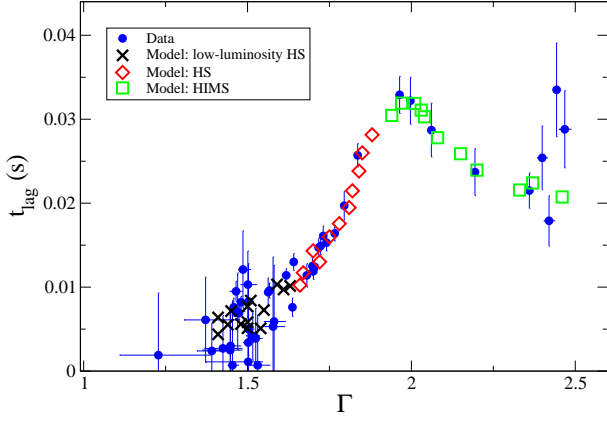


Fig. 2. Time lag of the 9 – 15 keV photons with respect to the 2 – 6 keV ones as a function of the spectral index Γ of the hard X-rays for the 2006-2007 outburst. The blue circles give the observations and the different symbols give the model results, as follows: black crosses - low-luminosity HS, red diamonds - HS, and green squares - HIMS.

taken to be in the hard state (HS, red diamonds in Fig. 2), and for $\Gamma \gtrsim 1.9$ the source is in the hard-intermediate state (HIMS, green squares in Fig. 2). Here, we follow the classification of Belloni (2010) of the spectral states of BHTs. To facilitate a comparison with the position of the source in the hardness-intensity diagram, we use the same symbols as in the middle panel of Fig. 1. We note that while the symbols represent the results of our model in Fig. 2, they correspond to the actual observations in Fig. 1 (top and middle panels).

To reproduce the observations, we have varied only two parameters, the radius R_0 of the jet at its base and the Thomson optical depth τ_{\parallel} along the axis of the jet. The rest of the parameters are kept at their reference values (Reig et al. 2018), namely $z_0 = 5r_g$, $H = 10^5 r_g$, $v_0 = 0.8c$, $\gamma = 2.24$, $z_1 = 50r_g$, $p = 0.5$, and $T_{bb} = 0.2$ keV. $r_g = GM/c^2$ is the gravitational radius. We assume a black-hole mass of $10 M_{\odot}$.

In Fig. 3, we show the values of the model parameters R_0 and τ_{\parallel} , that we have used in Fig. 2. We use the same symbols as in Fig. 2 for the three spectral states. We see several interesting results. a) For the transitions from the low-luminosity HS to the HS and HIMS, the Thomson optical depth τ_{\parallel} decreases monotonically from 11 to 2.25. b) For the same transitions, the radius R_0 of the base of the jet is not changing monotonically. From the initial stages of the outburst to the beginning of the HIMS R_0 increases, while for the rest of the HIMS R_0 decreases. We will offer a physical explanation for this behavior in § 5. c) More importantly, the parameters R_0 and τ_{\parallel} are correlated. Given the simplicity of our model, the match between observations and model is excellent and the values of the parameters R_0 and τ_{\parallel} are quite reasonable.

Another success of our model is the fact that it can reproduce qualitatively the correlation between the photon index of the power-law component and the break frequency ν_{br} of the radio spectrum, i.e., the frequency at which the entire jet becomes optically thin to synchrotron radiation (Koljonen et al. 2015). In BHTs, this break is expected in the IR region and could be related to the start of the particle acceleration in the jet (Polko et al. 2010). Fig. 4 shows ν_{br} as a function of Γ . The break frequency was calculated following Tsouros & Kylafis (2017) using the density of the electrons at the base of the jet and the radius of the jet there (for the jet models reported in Fig. 2) and assum-

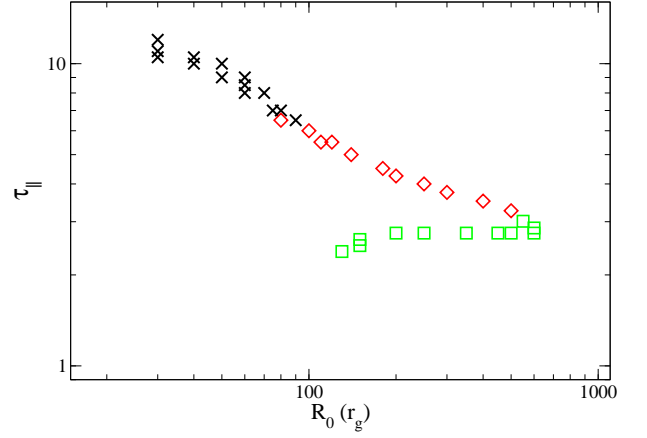


Fig. 3. Values of the parameters R_0 and τ_{\parallel} that correspond to the same models used in Fig. 2. The symbols are the same as in Fig. 2.

ing that the magnetic field at the base of the jet is $\sim 10^6$ Gauss (Giannios 2005). The scaling for the frequency is the minimum break frequency ν_{\min} obtained in the low-luminosity HS. The symbols are the same as in Fig. 2. The break frequency in the rise of the outburst should first increase and then decrease. The right branch of Fig. 4 agrees very well with the observations reported in Koljonen et al. (2015) who found that the photon index anti-correlates with the break frequency when the source transits from the HS to the HIMS (see Fig. 2 in that reference). Unfortunately, there are not good enough data to confirm the left branch, i.e. the dependence of the photon index on break frequency when the source moves along the hard state. Our model predicts a positive correlation between ν_{br} and Γ .

5. Discussion

The monotonic decrease of the optical depth τ_{\parallel} as Γ increases is naturally expected in all Comptonization models. Smaller optical depth means smaller number of scatterings and therefore a steeper power law. On the other hand, the initial increase and the later decrease of R_0 is more challenging to explain. Clearly, R_0 depends crucially on the poloidal magnetic field that is needed to eject the jet.

It is not easy to say what R_0 does as the luminosity of the source increases, if the magnetic field is advected inwards from far away and it is amplified on its way by random processes, such as turbulence. Fortunately, it was recently shown (Contopoulos et al. 2018) that the Cosmic Battery (Contopoulos & Kazanas 1998; Contopoulos et al. 2006) dominates over all random processes in the creation of poloidal magnetic fields in accreting black holes. Thus, we must use the Cosmic Battery to explain the dependence of R_0 on luminosity. There are no detailed calculations on this yet, thus by necessity we will offer a qualitative explanation. A quantitative one must be worked out and it will be done in the near future.

Since the poloidal magnetic field produced by the Cosmic Battery is proportional to luminosity (Kylafis et al. 2012), at the beginning of the HS, with the luminosity low, the created poloidal magnetic field is strong enough to eject a jet only near the Inner Stable Circular Orbit (ISCO). Thus, R_0 is of order several gravitational radii. As the luminosity increases, the strength of the poloidal magnetic field increases and R_0 also increases, but not indefinitely. This is because R_0 cannot increase beyond the transition radius R_{tr} , between the hot inner flow and the outer

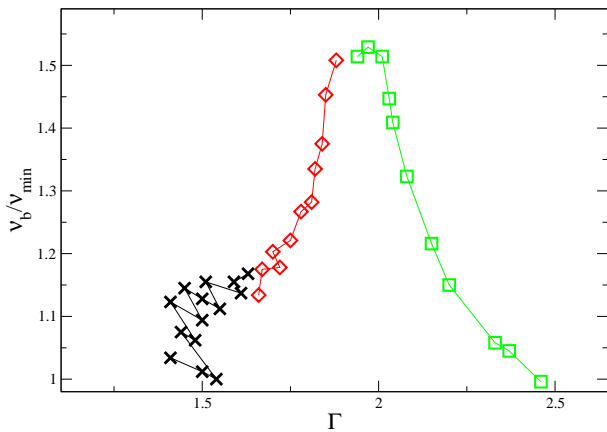


Fig. 4. Radio break frequency as a function of the photon index. The symbols are the same as in Fig. 1.

thin accretion disk (see Plant et al. 2015, for a recent determination of R_{tr}). Thus, somewhere at the beginning of the HIMS, R_0 reaches R_{tr} and after that it begins to decrease because R_{tr} decreases.

In Fig. 2, time flows from left to right. While the duration of the HS (red diamonds) is about 20 days, the time spent by the source in the HIMS (green squares) is less than 4 days. According to our model, the width of the jet reduces by a factor of ~ 3 in such a short time. At the same time, the optical depth (i.e. density) along the axis of the jet remains about the same (Fig. 3). A dramatic shrinking of the jet, while its central density remains unaffected, suggests that the jet quickly loses its outer parts. This could happen if the Shakura-Sunyaev disk moves inward quickly and “scythes” the jet. In other words, the extension of the thin disk inwards shrinks the hot inner flow that feeds the jet and the outer parts of the jet disappear, while its core remains more or less the same. This idea seems to be in agreement with the reduction of the disk truncation radius in the HIMS (Plant et al. 2015).

6. Conclusion

In our recent work (Reig et al. 2018), we found that BHTs as a class exhibit a correlation between the power-law photon index and the time lag between hard and soft photons. When considered as a whole (many sources), the correlation shows a large amount of scatter, because different sources seem to obey somewhat different correlations. Here, we have examined in detail this correlation for an individual source, namely, GX 339-4. We have found that the correlation is very tight. This correlation poses significant constraints on physical models of BHTs. We have shown that we can explain the correlation using our simple jet model and the Cosmic Battery. In addition, we make a prediction of how the break frequency of the radio spectrum should vary during the rising part of a large outburst.

Acknowledgements. We thank Ioannis Contopoulos for discussions regarding the Cosmic Battery and its effects on the size of the jet and Alexandros Tsouros for computing the break frequencies. We have also profited from useful discussions with Iossif Papadakis.

References

Altamirano, D. & Méndez, M. 2015, MNRAS, 449, 4027
 Arévalo, P. & Uttley, P. 2006, MNRAS, 367, 801
 Axelsson, M. & Done, C. 2018, ArXiv e-prints

Belloni, T. M. 2010, in Lecture Notes in Physics, Berlin Springer Verlag, Vol. 794, Lecture Notes in Physics, Berlin Springer Verlag, ed. T. Belloni, 53
 Böttcher, M. & Liang, E. P. 1999, ApJ, 511, L37
 Contopoulos, I. & Kazanas, D. 1998, ApJ, 508, 859
 Contopoulos, I., Kazanas, D., & Christodoulou, D. M. 2006, ApJ, 652, 1451
 Contopoulos, I., Nathanail, A., Sądowski, A., Kazanas, D., & Narayan, R. 2018, MNRAS, 473, 721
 Done, C., Gierliński, M., & Kubota, A. 2007, A&A Rev., 15, 1
 Dunn, R. J. H., Fender, R. P., Körding, E. G., Belloni, T., & Cabanac, C. 2010, MNRAS, 403, 61
 Esin, A. A., McClintock, J. E., & Narayan, R. 1997, ApJ, 489, 865
 Giannios, D. 2005, A&A, 437, 1007, “Paper III”
 Giannios, D., Kylafis, N. D., & Psaltis, D. 2004, A&A, 425, 163, “Paper II”
 Grinberg, V., Pottschmidt, K., Böck, M., et al. 2014, A&A, 565, A1
 Kalamkar, M., Reynolds, M. T., van der Klis, M., Altamirano, D., & Miller, J. M. 2015, ApJ, 802, 23
 Koljonen, K. I. I., Russell, D. M., Fernández-Ontiveros, J. A., et al. 2015, ApJ, 814, 139
 Kotov, O., Churazov, E., & Gilfanov, M. 2001, MNRAS, 327, 799
 Kroon, J. J. & Becker, P. A. 2016, ApJ, 821, 77
 Kylafis, N. D. & Belloni, T. M. 2015, A&A, 574, A133
 Kylafis, N. D., Contopoulos, I., Kazanas, D., & Christodoulou, D. M. 2012, A&A, 538, A5
 Kylafis, N. D., Papadakis, I. E., Reig, P., Giannios, D., & Pooley, G. G. 2008, A&A, 489, 481, “Paper IV”
 Markoff, S., Nowak, M. A., & Wilms, J. 2005, ApJ, 635, 1203
 Plant, D. S., Fender, R. P., Ponti, G., Muñoz-Darias, T., & Coriat, M. 2015, A&A, 573, A120
 Polko, P., Meier, D. L., & Markoff, S. 2010, ApJ, 723, 1343
 Pottschmidt, K., Wilms, J., Nowak, M. A., et al. 2003, A&A, 407, 1039
 Poutanen, J. & Fabian, A. C. 1999, MNRAS, 306, L31
 Reig, P. & Kylafis, N. D. 2015, A&A, 584, A109
 Reig, P., Kylafis, N. D., & Giannios, D. 2003, A&A, 403, L15, “Paper I”
 Reig, P., Kylafis, N. D., Papadakis, I. E., & Costado, M. T. 2018, MNRAS, 473, 4644
 Reig, P., Papadakis, I. E., Sobolewska, M. A., & Malzac, J. 2013, MNRAS, 435, 3395
 Shaposhnikov, N. & Titarchuk, L. 2009, ApJ, 699, 453
 Shidatsu, M., Ueda, Y., Yamada, S., et al. 2014, ApJ, 789, 100
 Stiele, H., Belloni, T. M., Kalemci, E., & Motta, S. 2013, MNRAS, 429, 2655
 Titarchuk, L. 1994, ApJ, 434, 570
 Tsouros, A. & Kylafis, N. D. 2017, A&A, 603, L4